ACS OMEGA

http://pubs.acs.org/journal/acsodf

Article

Photorefractive Response Enhancement in Poly(triarylamine)-Based Polymer Composites by a Second Electron Trap Chromophore

Naoto Tsutsumi,* Shintaro Sakamoto, Kenji Kinashi, Boaz Jessie Jackin, and Wataru Sakai

Cite This: *ACS Omega* 2022, 7, 12120−12126

Read Online

ACCESS | Metrics & More | Article Recommendations

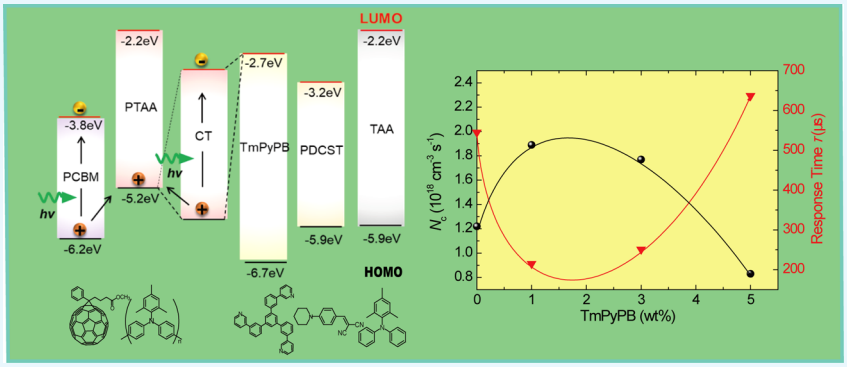

ABSTRACT: Photorefractive (PR) performances are affected by the components of the photoconductor, sensitizer, nonlinear optical dye, and plasticizer. A photoconductor with high hole mobility promises a faster response time, whereas it induces higher photoconductivity, which leads to easy dielectric breakdown. Adding a second electron trap is effective in controlling photoconductivity. In this study, the role of a second electron trap 1,3,5-tri[(3-pyridyl)-phen-3-yl]benzene (TmPyPB) was investigated in a PR composite consisting of a photoconductor of poly[bis(4-phenyl)(2,4,6-trimethylphenyl)amine] with a high hole mobility, a nonlinear optical chromophore of piperidinodicyanostyrene, a plasticizer of (2,4,6-trimethylphenyl)diphenylamine, and a sensitizer of [6,6]-phenyl C_{61} butyric acid-methyl ester. The minimum time response with the maximum optical diffraction efficiency and sensitivity was measured at a 1 wt % content of TmPyPB. These results were consistent with the number of charge carriers trapped per unit volume and per unit time N_c (cm^{-3} s^{-1}), which is defined as the ratio between the initial trap density T_i (cm^{-3}) and response time τ (s), at a 1 wt % content of TmPyPB. A faster response time of 149 μs, optical diffraction of 24.1% (external diffraction of 4.8%), and a sensitivity of 2746 cm^2 J^{-1} were measured at 50 V μm^{-1} for the sample with 1 wt % TmPyPB. High loading of 5 wt % TmPyPB led to a large decrease in photoconductivity and effectively suppressed the dielectric breakdown under a stronger electric field, whereas a slower response time with lower diffraction efficiency was observed for optical diffraction.

INTRODUCTION

Since photorefractive (PR) polymers were first investigated in 1991,[1] many studies have been reported to investigate and develop photorefractive polymers.[2−16] The essence of photorefractive polymers is the high optical diffraction efficiency and large optical gain based on the Pockels effect and molecular orientation of nonlinear optical dyes under the bias of the internally formed space-charge field and the external electric field. Furthermore, the photorefractive optical diffraction response time of triphenyl amine-based polymers is of the order of millisecond and submillisecond, which exceeds the video rate.[17,18] High optical diffraction and the large area size of PR polymer films enable holographic display applications.[13,16,19−23] Furthermore, the flexibility of the photorefractive films has an advantage of application in flexible devices.[24]

Poly[bis(4-phenyl)(2,4,6-trimethylphenyl)amine] (PTAA) with high hole mobility of 10^{-2}−10^{-3} cm^2 V^{-1} s^{-1} was developed in the electrophotonic field of organic transistors and organic solar cells. Due to high hole mobility, PTAA PR composites are expected to have faster response PR composites with high optical diffraction, but they also exhibit extremely large dark currents even though a relatively low electric field is applied, which induces a high risk of dielectric breakdown.[25] In our previous study,[25] a dramatic reduction in dark current was

Received: January 18, 2022
Accepted: February 8, 2022
Published: April 1, 2022

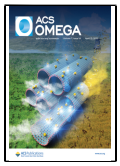

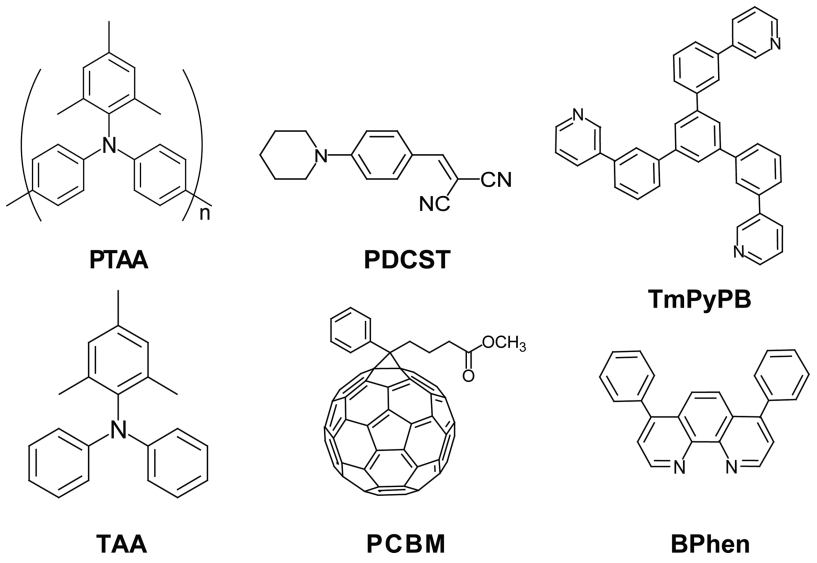

Figure 1. Structural formulae of compounds.

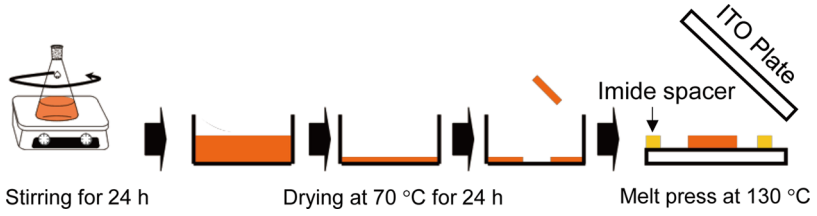

Figure 2. Schematic illustration to prepare the PR device.

achieved by introducing a self-assembled monolayer (SAM) onto an indium tin oxide (ITO) electrode with a Fermi level of −4.3 eV, which is 0.5 eV higher than that of ITO (−4.8 eV). The SAM layer prevents the electron flow from PTAA, whose highest occupied molecular orbital (HOMO) level is −5.2 eV, to the ITO electrode. The next issue to resolve was the high photoconduction at middle and high electric fields, which led to dielectric breakdown. The introduction of the second electron trap reagents, such as 4,7-diphenyl-1,10-phenanthroline (BPhen), 1,3-bis[2-(4-*tert*-butylphenyl)-1,3,4-oxadiazo-5-yl]benzene (OXD-7), and tris(8-hydroxyquinolinato)aluminum (Alq_3) reduced the photocurrent to improve the photorefractive responses.[17] PTAA photorefractive polymer with the second electron trap BPhen achieved a 397 μs response time with 50% optical diffraction efficiency.[17] Then, we aimed to seek the other second electron trap that would lead to a 100 μs response time.

In this report, we investigated the effect of another second electron trap of 1,3,5-tri[(3-pyridyl)-phen-3-yl]benzene (TmPyPB) on the photorefractive performances.

EXPERIMENTAL SECTION

Materials. A commercially available photoconductive polymer PTAA (Sigma-Aldrich) was used. Reprecipitation of PTAA was carried out as follows: PTAA dichloromethane solution was dipped into an excess amount of hexane with stirring. The yellow powder of PTTA was separated by centrifugation at 4000 rpm for 20 min. The yield was 94%. A plasticizer (2,4,6-trimethylphenyl)diphenylamine (TAA) and a nonlinear optical dye piperidinodicyanostyrene (PDCST) were used. Both chemicals were synthesized in our laboratory.[26] BPhen (Tokyo Kasei Co., Japan) and TmPyPB (Sigma-Aldrich) were employed as the second electron trap. [6,6]-Phenyl C_{61} butyric acid-methyl ester (PCBM) (Sigma-Aldrich) was employed as a sensitizer. Figure 1 summarizes the structural formulae of these compounds.

Sample Preparation. A schematic illustration of sample preparation is shown in Figure 2. The mixture of PTAA, 7-DCST, TAA, PCBM, and second trap reagent at a given weight % was dissolved in tetrahydrofuran and stirred for 24 h. After mixing, the solution was cast and then dried on a glass substrate at 70 °C for 24 h. The obtained PR sample was pressed between two pieces of ITO glass plate heated at 130 °C. The sample thickness was controlled with a 50 μm Teflon spacer. The obtained PR sample had thickness in the range of 50−60 μm.

Characterization. Absorption spectra in the ultraviolet and visible region were measured for the sample film using a Lambda 1050 ultraviolet/visible/near-infrared spectrophotometer (Perkin-Elmer). From the optical density (OD) measured, the absorption coefficient (α) was determined using the following equation

$$\mathrm{OD} = \varepsilon c d = \frac{\alpha d}{\ln 10} \quad (1)$$

where ε is the molar extinction coefficient, c is the molar concentration, and d is the sample thickness.

Photorefractive Measurements. The degenerate four-wave mixing method was employed to measure the diffraction efficiency and photorefractive response time. The laser source was a 25 mW DPSS laser at 532 nm (Samba, Cobolt AB, Sweden). The beam intensity was 0.534 W cm^{-2}. The sample

https://doi.org/10.1021/acsomega.2c00370
ACS Omega 2022, 7, 12120−12126

device was tilted at 50° to the sample normal. Two s-polarized writing beams were interfered in the sample film to form the modulation of the refractive index through both Pockels effect and orientation enhancement effect. The optical diffraction response was monitored using a counter-propagated p-polarized probe beam. A high-voltage amplifier (model 10/10E, TREK, Inc.) was employed to apply a rectangular high voltage at a 100 Hz frequency to the PR samples with a slew rate of 700 V μs^{-1}. With a current monitoring system of a TREK 10/10E, the photocurrent was simultaneously recorded.

The internal diffraction efficiency (η) was calculated as follows

$$\eta\ (\%) = \frac{I_d}{I_d + I_t} \times 100 \tag{2}$$

where I_t is the intensity of the transmitted probe beam and I_d is the intensity of the diffracted probe beam. The external diffraction efficiency (η_{ext}) was evaluated from the measured internal diffraction efficiency (η) as

$$\eta_{ext} = \exp\left(-\frac{\alpha d}{\cos\theta_1}\right)\eta \tag{3}$$

where θ_1 is the incidence angle of beam 1 inside the PR sample.

The rise time of optical diffraction was evaluated using a Kohlrausch−Williams−Watts equation

$$\eta = \eta_0\left\{1 - \exp\left[-\left(\frac{t}{\tau}\right)^{\beta}\right]\right\} \tag{4}$$

where τ is the response time, t is the time, η_0 is the steady-state diffraction efficiency, and β is a measure of the dispersion parameter that deviates from the single exponential behavior ($0 < \beta \leq 1$).

Optical gain (Γ) was measured with a two-beam coupling technique using a 532 nm p-polarized probe beam. Γ was evaluated using an equation of

$$\Gamma d = \cos\theta_1 \ln\left(\frac{I_1^t(I_2^t \neq 0)}{I_1^t(I_2^t = 0)}\right) - \cos\theta_2 \ln\left(\frac{I_2^t(I_1^t \neq 0)}{I_2^t(I_1^t = 0)}\right) \tag{5}$$

where θ_1 and θ_2 are the internal diffraction angles and I_1^t is the transmitted intensity of beam 1 and I_2^t is the intensity of beam 2.

Sensitivity (S) was evaluated as

$$S = \frac{\sqrt{\eta_{ext}}}{I\tau} \tag{6}$$

where I is the beam intensity.

RESULTS AND DISCUSSION

Photocurrent and Charge-Transfer (CT) Complex Formation. We focused on the relation between photocurrent and photorefractivity for photorefractive polymers.[17,18] Previous studies[17,18,27] have shown that the CT complex formed between the second electron trap and PTAA plays a significant role in the large reduction of photocurrent, which suppresses dielectric breakdown at middle and high electric fields.

The photocurrent is plotted against the electric field in Figure 3. The PR polymer composite with no second trap (blank) linearly increases the photocurrent up to E = 60 V μm^{-1}. However, the second electron trap of BPhen and

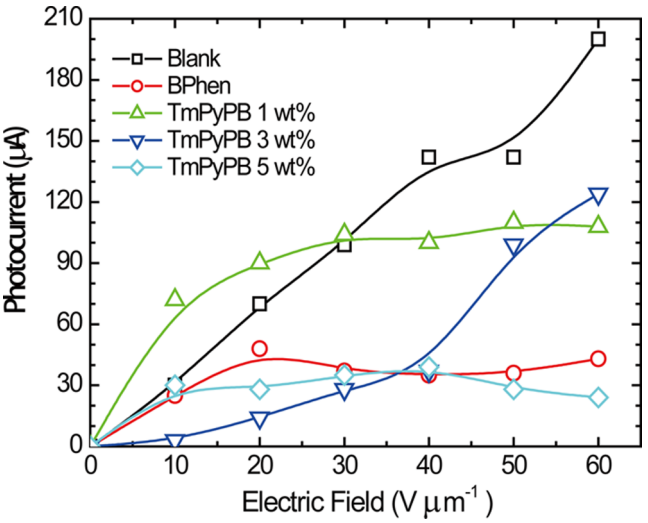

Figure 3. Plots of photocurrents vs electric fields for PR composites with and without the second trap chromophore.

TmPyPB significantly reduces the photocurrent of PR polymer composites. The photocurrent increased up to E = 20 V μm^{-1} for the PR polymer composite with the second trap, BPhen, and 1 and 5 wt % TmPyPB but leveled out above E = 20 V μm^{-1}. The PR polymer composite with 5 wt % TmPyPB shows a photocurrent of 24−30 μA, which is comparable to that for the PR polymer composite with the second trap BPhen.

The absorption spectra in the visible region are shown for PR polymer composites with and without the second trap of BPhen and TmPyPB in Figure 4. In a previous report,[17] the

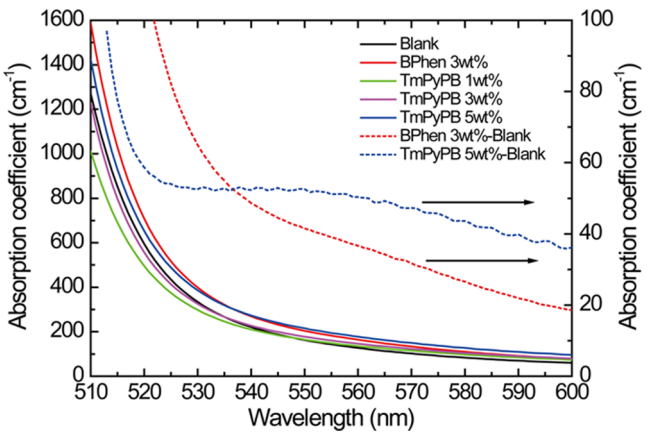

Figure 4. UV−vis absorption spectra for PR composites. Solid spectrum: measured spectrum. Dashed curve: differences in the spectra between BPhen 3 wt % and blank and that between TmPyPB 5 wt % and blank. The left scale is for solid spectrum. The right scale is for the dashed spectrum.

CT complex between BPhen and PTAA led to a significant reduction in the photocurrent. The energy-level diagram for the present PTAA-based polymer is shown in Figure 5. The present CT complex between PTAA and TmPyPB also plays a role in the significant reduction of photocurrent. The difference of the absorption spectra (blue dashed curve plotted against enlarged right scale in Figure 4) between composites with TmPyPB and the blank with no second trap is shown in Figure 4. The broad absorption around 560 nm is measured for the PR polymer composite with 5 wt % TmPyPB. Thus, the 5

https://doi.org/10.1021/acsomega.2c00370
ACS Omega 2022, 7, 12120−12126

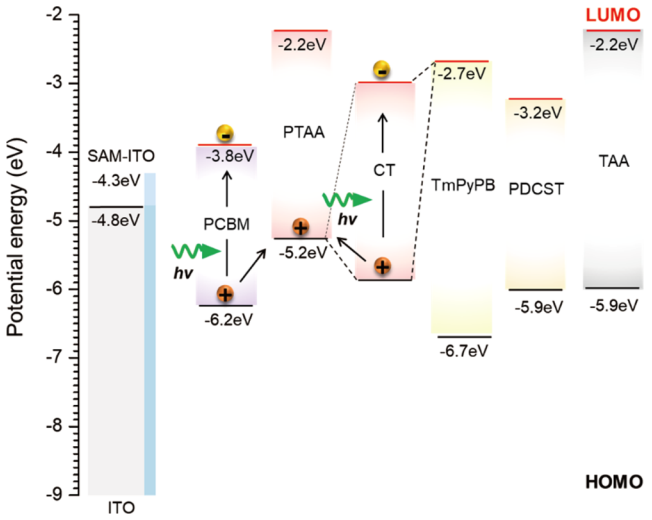

Figure 5. Diagram of the energy level in the present PR sample.

wt % TmPyPB loading significantly reduces the photocurrent through the CT complex, as shown in Figure 3. The same type of reduction in photocurrent was measured for the 1 and 3 wt % TmPyPB samples. In the next section, we discuss the effects of the TmPyPB content on the photorefractive quantities.

TmPyPB Content Dependence of Photorefractive Quantities. Figure 6 shows the rectangular response of

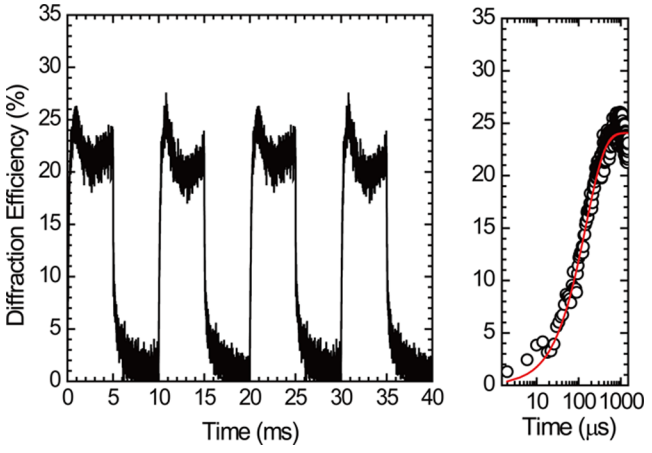

Figure 6. Left: repeating rectangular diffraction response for PTAA/PDCST/TAA/PCBM/TmPyPB (33.5/35/30/0.5/1 wt %) when a cycled rectangular electric field with a maximum of 50 V μm^{-1} is applied. Right: logarithmic time scale plots of diffraction efficiency. Observed diffraction efficiency is fitted well by the red curve with τ of 149 μs.

typical optical diffraction efficiency when a rectangular high voltage is turned on and off every 5 ms at 100 Hz. The effect of the content of TmPyPB on photorefractivity is important. Photorefractive quantities of η_{ext}, τ, and S measured at E = 60 V μm^{-1} are plotted with the TmPyPB content in Figure 7.

The maximum η_{ext} of 6.8% (internal one η of 34.2%) and S of 2267 $cm^2\ J^{-1}$ and the minimum τ of 215 μs are measured at the TmPyPB content of 1 wt %.

The question is why the addition of the second trap reagent of 1 wt % TmPyPB leads to better photorefractive performances, which can be compared with a previous study for the BPhen second trap case. In the case of BPhen, a 3 wt %

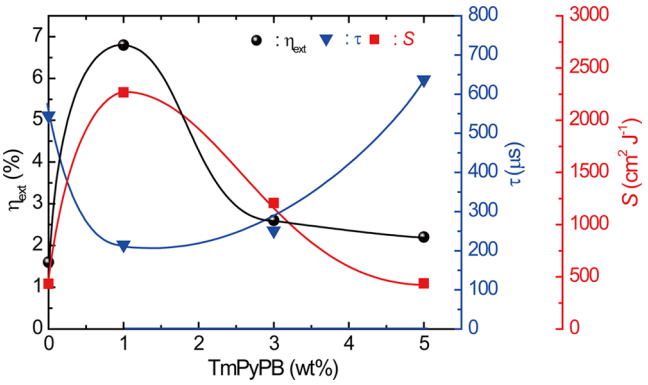

Figure 7. TmPyPB content dependence of η_{ext}, τ, and S in the PR composite at E = 60 V μm^{-1}. Solid curves are the guide to the eyes.

content of BPhen had the maximum sensitivity but a faster response time was reached at 1 wt % BPhen.[18]

Typical photocurrent and photorefractive quantities of Γ, η, η_{ext}, τ, and S measured at E = 60 V μm^{-1} for each PR composite are listed in Table 1.

The PR composite with 1 wt % TmPyPB gave η of 34.2% (η_{ext} of 6.8%), τ of 215 μs, and Γ of 106.5 cm^{-1}. The PR composite with 5 wt % TmPyPB showed η of 18.8% (η_{ext} of 2.6%), τ of 637 μs, Γ of 64.6 cm^{-1}, and photocurrent of 24 μA at E = 60 V μm^{-1}. The PR composite with 1 wt % TmPyPB achieved a high S of 2267 $cm^2\ J^{-1}$ due to faster τ of 215 μs and higher η_{ext} of 6.8%. τ became slower when the content of TmPyPB was increased. This might be related to the photocurrent. The photocurrent was significantly reduced for the sample with 5 wt % TmPyPB as shown in Figure 3. The photocurrent of 108 μA for 1 wt % TmPyPB and that of 124 μA for 3 wt % TmPyPB was largely reduced to 24 μA for 5 wt % TmPyPB. The lower photocurrent, i.e., lower photoconductivity, led to a slower response time, as discussed using eq 13.

Dependence of Photorefractive Quantities on the Electric Field. It is well known that the values of η, η_{ext}, τ, Γ, and S significantly depend on the electric field (E). Photorefractive quantities of η_{ext}, τ, and S are plotted with E for the PTAA composite with 1 wt % TmPyPB in Figure 8.

With increasing E, a monotonic increase in η_{ext}, a fast τ of 149 μs at E = 50 V μm^{-1}, and a resulting large value of S close to 3000 $cm^2\ J^{-1}$ are measured for the PTAA PR composite with 1 wt % TmPyPB.

Evaluation from Photocurrent. As discussed in previous papers,[17,18,25,26] based on the photocurrent measurements, the trap density T_i and trap limited space-charge field E_q are evaluated. The internal photocurrent efficiency $\varphi_{ph}(E)$ can be defined as follows with photocurrent per unit area J_{ph}[28,29]

$$\varphi_{ph}(E) = \frac{J_{ph} h\nu}{eI_0 \alpha d} = \frac{\sigma_{ph} E_0 h\nu}{eI_0 \alpha d} \quad (7)$$

where h is the Planck constant, ν is the optical frequency of the excited light, e is the electronic charge, I_0 is the light intensity per unit area, σ_p is the photoconductivity of the sample, and E_0 is the electric field. φ_{ph} was measured at E = 60 V μm^{-1} and is summarized in Table 2.

The photocarrier charge generation efficiency η_p is related to $\varphi_{ph}(E)$ with the photoconductivity gain factor G by eq 8[29]

https://doi.org/10.1021/acsomega.2c00370
ACS Omega 2022, 7, 12120−12126

Table 1. Thickness (d), Absorption Coefficient (α), Photocurrent (I_p), and PR Quantities for PTAA/PDCST/TAA/PCBM/Electron Trap = 34.5 − X/35/30/0.5/X at E = 60 V μm^{-1}

electron trap	X (wt %)	d (μm)	α (cm^{-1})	I_p (μA)	Γ (cm^{-1})	η (η_{ext}) (%)	τ (μs)	S (cm^2 J^{-1})
blank	0	56	303	200	na	10.2 (1.6)	545	434
BPhen	3	55	364	43	21.1	22.1 (2.5)	384	769
TmPyPB	1	54	275	108	106.5	34.2 (6.8)	215	2267
	3	58	299	124	110.7	17.4 (2.6)	251	1207
	5	55	356	24	64.6	18.8 (2.2)	637	437

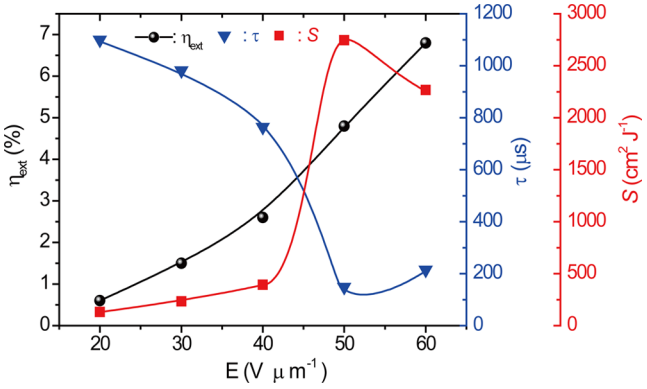

Figure 8. Electric field dependence of η_{ext}, τ, and the resulting S for PTAA/7-DCST/TAA/PCBM/TmPyPB (33.5/35/30/0.5/1 by wt). Solid curves are the guide to the eyes.

$$\varphi_{ph}(E) = G\eta_p = \frac{\varepsilon_r\varepsilon_0 E_0 \eta_p}{edT_i} \quad (8)$$

where ε_r is the relative dielectric constant, ε_0 is the vacuum permittivity, and T_i is the Schildkraut initial trap density.[30] ε_r = 3.5 measured[26] was used. G, η_p, and T_i values were calculated and are listed in Table 2.

Based on T_i = 5.42 × 10^{14} cm^{-3} for PTAA/PDCST/TAA/PCBM/BPhen = 33.5/35/30/0.5/1,[18] the G, η_p, and T_i values for other PR composites are evaluated under the assumption of $J_{ph} \propto \eta_p$.

E_q is estimated by eq 9 [29]

$$E_q = \frac{eT_i}{\varepsilon_r\varepsilon_0 K_G} \quad (9)$$

where the grating vector K_G is defined by $K_G = 2\pi/\Delta$, where Δ is the grating interval. E_{sc} is calculated using the model proposed by Kukhtarev[31,32] with E_q

$$E_{sc} = E_q\left(\frac{E_D^2 + E_p^2}{E_p^2 + (E_q + E_D)^2}\right)^{1/2} \quad (10)$$

where E_p is the electric field component projected onto the grating vector direction and E_D is the diffusion field ($E_D = K_G kT/e$, where T is the absolute temperature and k is the Boltzmann constant). The measured E_q and E_{sc} are listed in Table 2.

As shown in Table 2, E_q and E_{sc} are 0.95−1.27 V μm^{-1} and T_i is 4.08−5.42 × 10^{14} cm^{-3}, which cannot quantitatively explain the difference in photorefractive quantities in Table 1.

If all photogenerated charge carriers are trapped to contribute to the space-charge field formation, the diffraction response time τ_G is defined by the ratio between the initial trap density T_i and the total number of photogenerated charge carriers per unit volume and per unit time N_p (cm^{-3} s^{-1})[33]

$$\tau_G = \frac{T_i}{N_p} \quad (11)$$

where

$$N_p = \frac{\alpha\eta_p I_0}{h\nu} \quad (12)$$

From eqs 7, 8, 11, and 12, τ_G can be proportional to the inverse of photoconductivity σ_{ph}^{-1} as follows

$$\tau_G = \frac{\varepsilon_r\varepsilon_0}{\sigma_{ph}} \quad (13)$$

The calculated τ_G value is listed in Table 2.

The calculated value of τ_G for the samples with the second electron traps BPhen and TmPyPB is 3.8−7.7 times faster than the practically measured response time τ, whereas that for the blank is 27 times faster, as listed in Table 2. These results show that the photoconductivity is effectively reduced by the introduction of the second electron traps. A 5 wt % loading

Table 2. Photocurrent and Related Quantities for PTAA/PDCST/TAA/PCBM/Electron Trap = 34.5 − X/35/30/0.5/X at E = 60 V μm^{-1}

electron trap	X (wt %)	J_{ph} (A cm^{-2})	σ_{ph} (nS cm^{-1})	φ_{ph}	η_p	G	T_i (cm^{-3})	E_q/E_{sc} (V μm^{-1})
blank	0	0.00915	15.3	0.0235	0.0511	0.461	4.50 × 10^{14}	1.05/1.05
BPhen	3	0.00197	3.28	0.00429	0.0110	0.389	5.42 × 10^{14}	1.27/1.26
TmPyPB	1	0.00494	8.24	0.0145	0.0276	0.527	4.08 × 10^{14}	0.95/0.95
	3	0.00567	9.46	0.0143	0.0317	0.455	4.45 × 10^{14}	1.04/1.04
	5	0.00110	1.83	0.00245	0.0061	0.399	5.29 × 10^{14}	1.24/1.23

electron trap	X (wt %)	τ_G (μs)	N_p (cm^{-3} s^{-1})	τ (μs)	N_c (cm^{-3} s^{-1})
blank	0	20.3	2.21 × 10^{19}	545	1.22 × 10^{18}
BPhen	3	94.5	5.74 × 10^{18}	384	1.41 × 10^{18}
TmPyPB	1	37.6	1.08 × 10^{19}	215	1.89 × 10^{18}
	3	32.8	1.38 × 10^{19}	251	1.77 × 10^{18}
	5	169	3.12 × 10^{18}	637	0.83 × 10^{18}

https://doi.org/10.1021/acsomega.2c00370
ACS Omega 2022, 7, 12120−12126

of TmPyPB led to a significant reduction in photoconductivity, whereas it induced a slower response time. The response time τ is defined by the ratio between T_i and the number of charge carriers trapped per unit volume and per unit time N_c (cm^{-3} s^{-1})[18]

$$\tau = \frac{T_i}{N_c} \tag{14}$$

The faster response time is due to the increased number of N_c, as expected from eq 14. The value of N_c is plotted with the TmPyPB content in Figure 9. This result is consistent with the TmPyPB content dependence of the optical diffraction efficiency and sensitivity shown in Figure 7. A higher trapping rate leads to the space-charge formation, which is related to higher optical diffraction. N_c is a kind of relevant experimental parameter involving the photogenerated hole carriers, the hole transport through the hopping manifold, and the space-charge field for trapping. Larger carrier photogeneration, faster hole mobility, and larger space-charge field contribute to the increase in the N_c value.

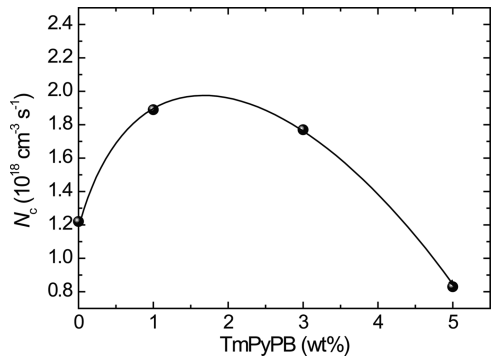

Figure 9. TmPyPB content dependence of the N_c value in the PTAA PR sample. The solid curve is the guide to the eyes.

CONCLUSIONS

The photorefractive performances and photoconductive properties of polymer composites consisting of PTAA, TAA, PDCST, PCBM, and the second electron trap of TmPyPB were investigated. Similar to the case with the BPhen second electron trap, TmPyPB formed a CT complex with PTAA, which effectively controlled the photoconductivity of the PTAA PR polymer composites. For the blank sample without the second trap, the photocurrent linearly increased with an applied electric field, whereas the loading of TmPyPB effectively suppressed the increase in photocurrent at $E \geq 20$ V μm^{-1}, which is effective in preventing dielectric breakdown at a high electric field. The loading of 1 wt % TmPyPB effectively increased the optical diffraction with a shortened response time and further loading of TmPyPB decreased the optical diffraction with a longer response time. The faster response time of 149 μs, external diffraction efficiency of 4.8% (internal diffraction of 24.1%), and sensitivity of 2746 cm^2 J^{-1} were measured for the sample with 1 wt % loading of TmPyPB at $E = 50$ V μm^{-1}.

The repeated measurement of the optical diffraction efficiency was monitored when the electric field was turned on and off at 100 Hz. The optical diffraction response time when the electric field was turned on was related to the formation of the space-charge field because the photogenerated carriers were trapped in traps, i.e., the redistributed photogenerated charge carriers along the grating with the applied electric field. N_c (cm^{-3} s^{-1}), which is defined a the ratio between T_i and the response time τ, is maximal at 1 wt % TmPyPB content, which is consistent with the TmPyPB content dependence of the diffraction efficiency and sensitivity.

AUTHOR INFORMATION

Corresponding Author

Naoto Tsutsumi − *Faculty of Materials Science and Engineering and Engineering, Kyoto Institute of Technology, Kyoto 606-8585, Japan;* orcid.org/0000-0001-8835-1347; Email: tsutsumi@kit.ac.jp

Authors

Shintaro Sakamoto − *Master Program of Innovative Materials, Graduate School of Science and Technology, Kyoto Institute of Technology, Kyoto 606-8585, Japan*

Kenji Kinashi − *Faculty of Materials Science and Engineering and Engineering, Kyoto Institute of Technology, Kyoto 606-8585, Japan;* orcid.org/0000-0003-4342-3516

Boaz Jessie Jackin − *Materials Innovation Laboratory, Kyoto Institute of Technology, Kyoto 606-8585, Japan*

Wataru Sakai − *Faculty of Materials Science and Engineering and Engineering, Kyoto Institute of Technology, Kyoto 606-8585, Japan;* orcid.org/0000-0002-0255-0861

Complete contact information is available at: https://pubs.acs.org/10.1021/acsomega.2c00370

Author Contributions

N.T. planned, directed, and coordinated the research. S.S. did the experiment. N.T., K.K., B.J.J., and W.S. discussed the research results. N.T. wrote the manuscript.

Notes

The authors declare no competing financial interest.

ACKNOWLEDGMENTS

This research was supported by the Strategic Promotion of Innovative Research and Development (S-innovation), Japan Science and Technology Agency (JST).

REFERENCES

(1) Ducharme, S.; Scott, J. C.; Twieg, R. J.; Moerner, W. E. Observation of the photorefractive effect in a polymer. *Phys. Rev. Lett.* **1991**, *66*, 1846−1849.

(2) Moerner, W. E.; Silence, S. M. Polymeric photorefractive materials. *Chem. Rev.* **1994**, *94*, 127−155.

(3) Zhang, Y.; Burzynski, R.; Ghosal, S.; Casstevens, M. K. Photorefractive polymers and composites. *Adv. Mater.* **1996**, *8*, 111−125.

(4) Moerner, W. E.; Grunnet-Jepsen, A.; Thompson, C. L. Photorefractive polymers. *Annu. Rev. Mater. Sci.* **1997**, *27*, 585−623.

(5) Zhang, Y.; Wada, T.; Sasabe, H. Carbazole photorefractive materials. *J. Mater. Chem.* **1998**, *8*, 809−828.

(6) Zilker, S. J. Materials design and physics of organic photorefractive systems. *ChemPhysChem* **2000**, *1*, 72−87.

(7) Wang, Q.; Wang, L.; Yu, L. Development of fully functionalized photorefractive polymers. *Macromol. Rapid Commun.* **2000**, *21*, 723−745.

(8) Kippelen, B.; Peyghambarian, N. Photorefractive Polymers and Their Applications. In *Polymers for Photonics Applications II*; Springer: Berlin, Heidelberg, 2003; Vol. *161*, pp 87−156.

https://doi.org/10.1021/acsomega.2c00370
ACS Omega 2022, 7, 12120−12126

(9) Ostroverkhova, O.; Moerner, W. E. Organic photorefractives: mechanisms, materials, and applications. *Chem. Rev.* **2004**, *104*, 3267−3314.
(10) Sasaki, T. Photorefractive effect of liquid crystalline materials. *Polym. J.* **2005**, *37*, 797−812.
(11) Thomas, J.; Norwood, R. A.; Peyghambarian, N. Nonlinear optical polymers for photorefractive applications. *J. Mater. Chem.* **2009**, *19*, 7476−7489.
(12) Köber, S.; Salvador, M.; Meerholz, K. Organic photorefractive materials and applications. *Adv. Mater.* **2011**, *23*, 4725−4763.
(13) Lynn, B.; Blanche, P.-A.; Peyghambarian, N. Photorefractive polymers for holography. *J. Polym. Sci., Part B: Polym. Phys.* **2014**, *52*, 193−231.
(14) Tsutsumi, N. Molecular design of photorefractive polymers. *Polym. J.* **2016**, *48*, 571−588.
(15) Tsutsumi, N. Recent advances in photorefractive and photoactive polymers for holographic applications. *Polym. Int.* **2017**, *66*, 167−174.
(16) Blanche, P.-A.; Ka, J.-W.; Peyghambarian, N. Review of Organic Photorefractive Materials and Their Use for Updateable 3D Display. *Materials* **2021**, *14*, No. 5799.
(17) Masumura, K.; Oka, T.; Kinashi, K.; Tsutsumi, N.; et al. Photorefractive dynamics in poly(triarylamine)-based polymer composite: An approach utilizing a second electron trap to reduce the photoconductivity. *Opt. Mater. Express* **2018**, *8*, 401−412.
(18) Masumura, K.; Nakanishi, I.; Van Thi Khuat, K. V.; Kinashi, K.; Sakai, W.; Tsutsumi, N. Optimal composition of the poly-(triarylamine)-based polymer composite to maximize photorefractive performance. *Sci. Rep.* **2019**, *9*, No. 739.
(19) Blanche, P.; Tay, S.; Voorakaranam, R.; Saint-Hilaire, P.; Christenson, C.; Gu, T.; Lin, W.; Flores, D.; Wang, P.; Yamamoto, M.; Thomas, J.; Norwood, R. A.; Peyghambarian, N. An updatable holographic display for 3D visualization. *J. Disp. Technol.* **2008**, *4*, 424−430.
(20) Blanche, P.-A.; Bablumian, A.; Voorakaranam, R.; Christenson, C.; Lin, W.; Gu, T.; Flores, D.; Wang, P.; Hsieh, W.-Y.; Kathaperumal, M.; Rachwal, B.; Siddiqui, O.; Thomas, J.; Norwood, R. A.; Yamamoto, M.; Peyghambarian, N. Holographic three-dimensional telepresence using large-area photorefractive polymer. *Nature* **2010**, *468*, 80−83.
(21) Tsutsumi, N.; Kinashi, K.; Nonomura, A.; Sakai, W. Quickly Updatable Hologram Images Using Poly(N-vinyl Carbazole) (PVCz) Photorefractive Polymer Composite. *Materials* **2012**, *5*, 1477−1486.
(22) Tsujimura, S.; Kinashi, K.; Sakai, W.; Tsutsumi, N. High-speed photorefractive response capability in triphenylamine polymer-based composites. *Appl. Phys. Express* **2012**, *5*, No. 064101.
(23) Giang, H. N.; Kinashi, K.; Sakai, W.; Tsutsumi, N. Photorefractive response using composite based on poly(4-(diphenylamino)benzyl acrylate) and real-time holographic application. *Polym. J.* **2014**, *46*, 59−66.
(24) Kinashi, K.; Matsumura, M.; Sakai, W.; Tsutsumi, N. Flexible All-Organic Photorefractive Devices. *ACS Appl. Electron. Mater.* **2019**, *1*, 238−245.
(25) Kinashi, K.; Shinkai, H.; Sakai, W.; Tsutsumi, N. Photorefractive device using self-assembled monolayer coated indium-tin-oxide electrodes. *Org. Electron.* **2013**, *14*, 2987−2993.
(26) Tsutsumi, N.; Kinashi, K.; Masumura, K.; Kono, K. Photorefractive performance of poly(triarylamine)-based polymer composites: An approach from the photoconductive properties. *J. Polym. Sci., Part B: Polym. Phys.* **2015**, *53*, 502−508.
(27) Tsutsumi, N.; Kinashi, K.; Masumura, K.; Kono, K. Photorefractive dynamics in poly (triarylamine)-based polymer composites. *Opt. Express* **2015**, *23*, 25158−25170.
(28) Chantharasupawong, P.; Christenson, C. W.; Philip, R.; Zhai, L.; Winiarz, J.; Yamamoto, M.; Tetard, L.; Nair, R. R.; Thomas, J. Photorefractive performances of a graphene-doped PATPD/7-DCST/ECZ composite. *J. Mater. Chem. C* **2014**, *2*, 7639−7647.
(29) Däubler, T. K.; Bittner, R.; Meerholz, K.; Cimrová, V.; Neher, D. Charge carrier photogeneration, trapping, and space-charge field formation in PVK-based photorefractive materials. *Phys. Rev. B* **2000**, *61*, 13515−13527.
(30) Schildkraut, J. S.; Buettner, A. V. Theory and simulation of the formation and erasure of space charge gratings in photoconductive polymers. *J. Appl. Phys.* **1992**, *72*, 1888−1893.
(31) Kukhtarev, N. V.; Markov, V. B.; Odulov, S. G.; Soskin, M. S.; Vinetskii, V. L. Holographic storage in electrooptic crystals. I. Steady state. *Ferroelectrics* **1978**, *22*, 949−960.
(32) Kinashi, K.; Wang, Y.; Sakai, W.; Tsutsumi, N. Optimization of photorefractivity based on poly(Nvinylcarbazole) composites: An approach from the perspectives of chemistry and physics. *Macromol. Chem. Phys.* **2013**, *214*, 1789−1797.
(33) Däubler, T. K.; Kulikovsky, L.; Neher, D.; Cimrová, V.; Hummelen, J. C.; Mecher, E.; Bittner, R.; Meerholz, K. Photoconductivity and Charge-Carrier Photogeneration in Photorefractive Polymers. In *Nonlinear Optical Transmission Processes and Organic Photorefractive Materials*; International Society for Optics and Photonics, 2002; pp 206−216.

https://doi.org/10.1021/acsomega.2c00370
ACS Omega 2022, 7, 12120−12126